NASA

Technical Memorandum 85067

Infrared Molecular Emissions from Comets

H. A. Weaver and M. J. Mumma

JULY 1983

National Aeronautics and
Space Administration

Goddard Space Flight Center
Greenbelt, Maryland 20771

ABSTRACT

Until recently, IR observations of comets have consisted mainly of low resolution photometric measurements of grain (dust) radiation. The present paper explores the possibility of detecting IR molecular line emission from cometary parent molecules. Due to the non-LTE conditions in the inner coma and the large amount of near IR solar flux, IR fluorescence will be a significant source of cometary emission and, in fact, will dominate the grain radiation in a sufficiently high resolution instrument. The detection of this line emission will be difficult due to absorption in the terrestrial atmosphere, but it appears possible to measure cometary H_2O emission from airplane altitudes ($\sim$12 km). As IR molecular line emission represents one of the few promising methods of detecting cometary parent molecules directly, further research on this problem should be vigorously pursued.

Subject headings: comets -- infrared: spectra -- molecular processes

PRECEDING PAGE BLANK NOT FILMED

I. Introduction

Infrared (IR) observations of comets have generally been made using filter photometry. Acquired at low spectral resolution ($\lambda/\Delta\lambda \lesssim 100$), these studies provide data primarily on the cometary grains (dust), which are small (typically micron size but sometimes larger) solid particles dragged away from the nucleus by the subliming "parent" molecules (constituents of the nucleus which leave in the gas phase). Except for the so-called "silicate features" at $\sim$10 μm and $\sim$18 μm, the IR radiation from the grains is primarily thermal (i.e., greybody in nature), so that photometry is well suited for the study of grain properties. IR photometry of bright comets is reviewed by Ney (1982), and of faint periodic comets by Campins and Hanner (1982).

This paper is concerned with IR cometary radiation which is of a completely different nature from that described above, and whose detection and characterization will, in general, require observations at a higher spectral resolution than filter photometry can provide. We investigate the possible existence of IR molecular line emissions in comets. In particular, we investigate whether or not there will be detectable IR molecular emissions from the cometary parent molecules. Since many of the proposed parent molecules have strong ro-vibrational transitions in the IR (e.g., H_2O, CO_2, CO, NH_3, CH_4,....), and since some of these do not fluoresce in the visible or ultraviolet (UV) spectral ranges (e.g., H_2O, CO_2, NH_3, CH_4,...), and others do not have electric dipole allowed rotational transitions (e.g., CO_2, CH_4,...), the IR becomes a prime candidate spectral region for the discovery and study of these molecules.

IR molecular emissions have already been detected in comet West (see

Johnson, Fink, and Larson 1983), but these emissions were from electronic transitions of "fragment" molecules (molecules which do not reside, as such, in the nucleus but are created in the coma, for example, by photodissociation of parent molecules). The physics of these emissions is therefore very similar to the physics of visible or UV cometary emissions. In contrast, we discuss the production of IR molecular emissions due to ro-vibrational transitions in cometary parent molecules. The molecules we have chosen to investigate are H_2O, CO_2, CO, and NH_3. These molecules do not form a complete set of possible cometary parent molecules, but they serve the purpose of illustrating basic principles presented in this paper. Furthermore, since H_2O is generally considered to be the most important (i.e., most abundant) molecular constituent of the cometary nucleus, while CO_2 and CO are regarded as particularly important in some "new" (i.e., long period or non-periodic) comets (see Delsemme 1982 for a review), we have attempted to be realistic in our choice. Although NH_3 is no longer considered to be very abundant in the nucleus ($\lesssim$1% by number), it was proposed as an important constituent in early comet models (Whipple 1950 and 1951) and continues to be used as a constituent of hypothetical models of cometary nuclei (Huebner and Giguere 1980; Mitchell, Prasad, and Huntress 1981; Swift and Mitchell 1981; Biermann, Giguere, and Huebner 1982). Laser heterodyne spectroscopy may be a sensitive technique for the detection of cometary NH_3, and since we will use this technique to search for NH_3 in bright comets, we have included NH_3 in the list of molecules to be considered here.

We have also decided to include ro-vibrational transitions of OH in our study. Although OH itself has never been proposed as a constituent of the nucleus, its presence in the coma is generally considered to be a tracer for H_2O. OH has already been observed in many comets in the UV and radio regions

(see Feldman 1982 and Despois et al. 1981 for a discussion), so it is interesting to consider its possible IR emissions. Numerous fluorescence calculations have been made for OH to interpret its UV and radio emissions (Hunaerts 1953; Dossin et al. 1961; Biraud et al. 1974; Mies 1974a; Lane, Stockton, and Mies 1974; Despois et al. 1981; Schleicher and A'Hearn 1982). The most recent calculation (Schleicher and A'Hearn 1982) appears to be the most accurate since it is based upon a significantly improved solar spectrum and more molecular transitions, compared with earlier formulations. However, none of these previous works have included IR pumping and thus they may significantly underestimate the amount of IR emission. Part of the motivation for including OH in the present study is to demonstrate the importance of IR pumping in producing excitation in cometary molecules.

This paper is organized as follows. First, we consider in a general way the physical processes operating in the inner coma of a comet. Parent molecules are most abundant in this region and, hence, the inner coma will be the primary source of their emission. Next, we discuss specific molecules to determine the regions in the coma where local thermodynamic equilibrium (LTE) is not valid. We then demonstrate that scattering of solar radiation can be a significant source of IR molecular line emission when LTE is not maintained. For this case, we discuss excitation rates for IR fluorescence and estimate the brightnesses of IR molecular line emissions from a representative moderately-bright comet. Finally, we summarize our results, discuss their significance, and comment on the future role of IR observations of comets.

Concerning previous work in this area, a literature search reveals that a virtual void previously existed. The present paper is actually an extension of

earlier work by one of us (Mumma 1980), which to our knowledge is the first attempt to explain IR cometary molecular emission by addressing the non-LTE effects which are principally responsible for these emissions. Recently, Yamamoto (1982) presented calculations for the fluxes expected from various possible cometary molecules in the IR. His paper is a useful treatment of this subject, but he gives virtually no details concerning his calculations and he generally neglects many of the points considered in the present paper. For example, Yamamoto assumes that molecular line radiation in the coma is due to IR fluorescence, implying that vibrational LTE is not valid. On the other hand, he assumes that the lines within the vibrational bands follow a thermal distribution, implying that rotational LTE is maintained. Since neither assumption is obviously valid throughout the coma, each requires detailed discussion. Even more recently, a French group (Encrenaz et al. 1982; Crovisier 1982) has presented, in a preliminary fashion, some results of an analysis they have performed to estimate the IR emissions from comet Halley. The only molecule for which they give any detail is H_2O, and, in this case, their results appear to be consistent with our own.

II. General Considerations

Fig. 1 shows the IR flux from comet Bennett (1970 II) measured by Ney (1974) using filter photometry. As discussed earlier, the dominant component of this observed flux is thermal radiation from cometary grains. Also indicated in Fig. 1 are the positions of the vibrational transitions considered in this paper. The presence of a strong internal source of IR radiation raises the interesting possibility of detecting parent molecules in the IR by their absorption of thermal dust continuum. However, collisional relaxation does not

compete favorably with radiative vibrational relaxation in the cometary coma, implying that each photon absorbed from the thermal dust continuum is re-emitted (see Sec. III). Since both grains and gas are isotropic emitters, and since they have similar spatial distributions, the surface brightness is unchanged in the spectral line. Neglecting branching ratio effects, it appears that cometary parent molecules cannot be detected by absorption lines in the IR.

Cometary atoms and molecules are detected in visible and UV spectra by their emission lines, which are usually produced by fluorescence in the solar radiation field ([OI] is an important exception). The solar flux (Fig. 1; Labs and Neckel 1968) actually peaks in the near IR ($\lambda \sim 1.6$ μm) suggesting that IR fluorescence may provide a means of detecting cometary parent molecules if they re-emit the absorbed solar radiation before collisional (or other) de-excitation occurs. However, it is not obvious that fluorescence will be important for IR transitions since the competition between radiative and collisional processes is much keener there than in the UV or visible. Collision cross sections generally grow for decreasing energy separations of the levels involved in transitions, while spontaneous radiative transition probabilities usually decrease under the same circumstances. Thus, even though collisions are unimportant for most UV and visible transitions, they may still play an important role in some IR transitions, and this role must be determined individually for each molecule.

If LTE is maintained in the coma, then IR fluorescence in the solar radiation field will not occur, because of quenching by collisions. Under these circumstances, the IR radiation from the molecules in the coma will be primarily thermal in nature. This is not necessarily a drawback with regard to the observation of IR molecular line emission. For example, a simple calculation

demonstrates that the ν_2 level of CO_2 (which is 667 cm^{-1} above the ground level) would have a significantly higher population under the conditions of vibrational LTE at a temperature of 200 K than it would have if the level were in fluorescence equilibrium. The reverse situation prevails (i.e., larger population in fluorescence equilibrium) for levels having larger excitation energies (which prevents easy thermal excitation) and for which a larger amount of solar flux is available for fluorescence. In fact, for all of the other IR bands considered in this paper, the IR emission will be significantly enhanced when vibrational LTE is not maintained.

The relative importance of collisional and radiative effects may be assessed by examining the rate equation for an excited energy level. A general rate equation taking into account all possible physical processes would be hopelessly complicated. Fortunately, considerable simplification is made possible by eliminating those effects which are expected to be unimportant in the cometary coma.

We will not consider a time-dependent rate equation. Following Arpigny (1964), the excitation and de-excitation rates considered here will generally be large enough that the molecules will at least approach the steady state condition. A probable exception is CO, due to its relatively long rotational radiative lifetimes. Preliminary results for CO indicate that the relative vibrational populations are equilibrated very quickly, but the distribution among the rotational levels may never reach steady state in the observable coma (Weaver and Chin, private communication (1983)). The rotational distributions used for our calculations are discussed in Section IV.

Excepting homonuclear molecules (e.g., C_2, H_2), we expect nearly all molecules to be in the lowest vibrational level of the ground electronic state. Thus, for both collisional and radiative processes, we assume that at least one of the interacting levels is in this state.

Restricting interactions to those connecting the excited level and the ground state only, eliminates from the discussion a mechanism we term "Franck-Condon pumping," which can produce significant IR emissions. In this process, molecules excited by resonance electronic transitions in the visible or UV spectral regions may be left in higher vibrational states upon returning to the ground electronic state. These high vibrational levels will subsequently decay by vibrational cascade, accompanied by the emission of IR radiation. For favorable cases many IR photons will be emitted for each UV or visible photon absorbed, thereby producing larger photon emission rates in the IR than in the UV or visible. In general, a mismatch in the mean bond-lengths for the upper and lower electronic states will result in a Franck-Condon envelope which is extended over several vibrational levels, and vibrational pumping will result for such molecules. For example, the CN ($A\ ^2\pi - X\ ^2\Sigma^+$) red system has a wide Franck-Condon envelope and fluorescence in this system will produce extensive vibrational pumping, and, consequently, large IR emissions. Although Franck-Condon pumping works well for most diatomic molecules, it will not be as important for polyatomic molecules because their upper electronic states usually pre-dissociate.

Stimulated emission and optical trapping effects are neglected in the rate equation. A quick calculation demonstrates that stimulated emission is certainly unimportant for the vibrational transitions considered, and is

probably unimportant for the rotational transitions as well. In the inner coma, where the column densities are highest, fairly large optical depths (>>1) may be encountered in the cores of the strongest ro-vibrational transitions of some parent molecules. When significant radiative trapping occurs, a resonance photon may be scattered many times before exiting the coma, and it has a correspondingly higher probability of being thermalized. This phenomenon lowers the "effective" Einstein A value for the transition and allows LTE to be maintained at a lower density than would have been required in the optically thin case. This effect plays an important role in the analysis of non-LTE processes in the mesospheres of Mars and Venus (Deming and Mumma 1983; Dickinson 1972, 1976) and may be important in comets. We include optical depth effects later in the discussion of IR fluorescence (section IV), but we will neglect optical trapping in determining where in the coma the assumption of LTE is not valid.

Only neutral-neutral collisions producing energy exchange between translational and vibrational (T-V process) or rotational (T-R process) modes are considered. Collisions transferring vibrational energy of one species into vibrational energy of the same or other species (V-V process) may be important for high excitation energy vibrational modes, but we will not consider this process. Excitation and de-excitation of neutral molecules can also occur by collisions with ions and electrons (electrons being the most important). Although fairly high electron densities may be present in the inner coma ($n_e \gtrsim 10^4$ cm^{-3} according to Giguere and Huebner 1978), we feel that not enough quantitative information is available to consider this process realistically here.

We also neglect direct production of molecules in excited states. For example, some parent molecules leave the nucleus with thermal excitation and may relax radiatively as they flow into the coma. Calculations indicate that this will not be a significant source of emission for the transitions considered here. It is also possible that CO is a photodissociation product and, thus, may be produced in an excited state (e.g., in the photodissociation of CO_2 (Huebner and Carpenter 1979)). Highly excited rotational states of OH are produced in the photodissociation of H_2O by H Ly α photons (Yamashita 1975). Since we are concentrating on parent molecules, we neglect such effects.

Thus, we write the following simplified rate equation:

$$dn_u/dt = 0 = n_\ell(B_{\ell u}\,\rho + C_{\ell u}) - n_u\,(A_{u\ell} + C_{u\ell}) \qquad (1)$$

where, n_ℓ, n_u ≡ number densities in the lower and upper energy levels, respectively, of the effective two level system,

ρ ≡ density of the radiation field at the position of the molecule and at the frequency of the transition,

$B_{\ell u}$ ≡ Einstein coefficient for stimulated absorption,

$A_{u\ell}$ ≡ Einstein coefficient for spontaneous emission,

and $C_{\ell u}$, $C_{u\ell}$ ≡ collisional excitation and relaxation rates, respectively.

Equation (1) is an acceptably accurate and tractable description of the physics in the inner coma, enabling us to discuss our ideas concerning the production of IR molecular emissions quantitatively. Processes not included explicitly are assumed to produce relatively small effects and can be included in future, more detailed studies.

We next consider (separately) vibrational transitions in the near to middle IR and rotational transitions which occur at much longer wavelengths. We treat the former in order to estimate the integrated IR brightnesses of vibrational bands. We treat the latter because these transitions help determine the population distribution among the various rotational levels of the ground state, and, hence, the intensity distribution within the vibrational bands. For vibrational transitions, n_ℓ will represent the lowest energy vibrational level, while n_u will be an excited vibrational level. For rotational transitions, n_ℓ and n_u will refer to energy levels within the lowest energy vibrational level (for radiative transitions this will mean energy levels with total angular momentum quantum numbers differing by one unit).

The collisional excitation and relaxation rates are given by:

$$C_{\ell u} \equiv n_T \sigma_\uparrow \bar{v} \tag{2}$$

and

$$C_{u\ell} \equiv n_T \sigma_\downarrow \bar{v} \tag{3}$$

where $n_T \equiv$ total gas number density (cm^{-3}),

$\sigma_\uparrow, \sigma_\downarrow \equiv$ excitation and relaxation cross sections (cm^2),

respectively, for the (T-V) or (T-R) collisions connecting the levels considered,

and $\bar{v}$ ≡ average relative speed of the colliding molecules.

Using the detailed balance condition, equation (1) can be rewritten as:

$$n_u/n_\ell = (g_u/g_\ell)(e^{-(hc\nu/kT)})[(1+B_{\ell u}\rho/C_{\ell u})/(1+A_{u\ell}/C_{u\ell})] \qquad (4)$$

where, T ≡ local kinetic temperature (K),

and ν ≡ wavenumber of the transition (cm^{-1}).

From equation (4) we see that a sufficient condition for LTE is:

$$B_{\ell u}\rho/C_{\ell u} \ll 1 \quad \underline{\text{and}} \quad A_{u\ell}/C_{u\ell} \ll 1$$

In other words, LTE is maintained in the inner coma when collisions dominate radiative processes (Notice that setting $(1+B_{\ell u}\rho/C_{\ell u})=(1+A_{u\ell}/C_{u\ell})$ yields another sufficient condition for LTE. However, this condition simply implies that LTE is valid when the radiation field is identical to that of a blackbody whose temperature is equal to the kinetic temperature of the coma).

It is clear that radiative excitation plays an important role in the excitation of vibrational transitions. However, the different spectral character of the solar and grain radiation fields raises the interesting question: which source dominates the local radiation field in the 10 μm

spectral region at the position of the comet? The temperature of a typical cometary grain at R (≡ heliocentric distance of comet) = 1 a.u. is ∿330 K (following Ney (1974), this is ∿20% larger than the temperature of a blackbody at this distance from the sun). The radiation density near 10 μm of a blackbody at T = 330 K is approximately three orders of magnitude larger than the corresponding density of the solar radiation field at 1 a.u. However, the radiation density due to the grains will not be equal to that of a blackbody at the same temperature as the grains for two reasons. First, the grains are not "black"; they have an emissivity less than one and their emissivity changes with wavelength (Ney 1974). More importantly, since the grains do not completely fill the region around the nucleus (i.e., they form a very tenuous "atmosphere"), the grain radiation field is diluted from the blackbody value. For example, Ney (1974) estimates for comet Bennett (1970 II) that the average grain optical depth is $\sim 10^{-4}$-10^{-5} in a field of view subtending ∿7000 km at the comet, producing a dilution factor of this same order. We calculate that for wavelengths longward of ∿10μm, the grain radiation field will be stronger than the solar field for a region within ∿500 km of the nucleus. Nevertheless, for the IR vibrational transitions considered here, we consider only fluorescence produced by the solar field. Under these conditions we have:

$$B_{\ell u} \rho = g_{band} \tag{5}$$

where g_{band} ≡ excitation factor or "g-factor" for the vibrational band (photons s^{-1} $molecule^{-1}$).

The concept of the g-factor is extensively discussed in section IV when we consider IR fluorescence.

If the total number density is taken to be that of H_2O and a Haser model (Haser 1966; the validity of the Haser model is discussed by Festou 1981) is used to determine the H_2O density, then:

$$n_T = (Q_{H_2O}/4\pi r^2 v')e^{-(r/v'\tau)} \qquad (6)$$

where, Q_{H_2O} ≡ H_2O production rate (molecules s^{-1}),

r ≡ radial distance to the center of the nucleus,

v' ≡ radial outflow velocity for the H_2O molecules (assumed to be the same value for all H_2O molecules),

and τ ≡ H_2O lifetime.

For H_2O, $v'\tau \sim 4\text{-}8 \times 10^4$ km at R = 1 a.u. (Weaver et al. 1981) so that the exponential term may be safely neglected within a few thousand kilometers of the nucleus.

We now define the "disequilibrium distance", $D_\dagger$, as the distance from the nucleus outside of which collisions will be of minor importance in producing vibrational excitation. We calculate $D_\dagger$ by setting the radiative excitation rate equal to the collisional rate. Using equations (2), (5), and (6) (but neglecting the exponential factor in (6)), the disequilibrium distance can be written as:

$$D_\dagger = (Q_{H_2O}\sigma_\dagger/4\pi g_{band})^{1/2} (\bar{v}/v')^{1/2} \qquad (7)$$

The temperature of an H_2O-ice nucleus changes very little with heliocentric distance when R < 2 a.u. because virtually all the incident solar energy goes into sublimation and little is available for surface heating (Weissman and Kieffer 1981). The temperature attained by the nucleus depends on factors such as albedo, heat transport parameters, etc., but "reasonable" values for all these parameters yield temperatures of ∿200 K. The kinetic temperature of the sublimed gases will initially decrease with increasing distance from the nucleus due to expansion. Photodissociation heats the coma, but probably not by enough to overcome the expansion cooling (at least in the inner coma). These conclusions are supported by the calculations of Shimizu (1976) and Marconi and Mendis (1982). Besides expansion cooling and photochemical heating, these authors have also included radiative cooling by pure rotational transitions of H_2O. They find that the kinetic temperature decreases from a value of ∿200 K at the surface of the nucleus to ∿10 K at ∿100 km from the nucleus, followed by a monotonically rising temperature for larger distances from the nucleus. However, we will assume that the temperature of the nucleus (T=200 K) also defines the kinetic temperature of the gas throughout the inner coma. We simply note that the processes not considered here will probably shrink the disequilibrium distance to a smaller value than we calculate. Furthermore, by analogy with work done for interstellar clouds (Nuth and Donn 1981), considerable departures from LTE can be expected well within the radius at which the collisional and radiative rates are equal.

Under our assumptions, the average relative thermal speed of the colliding coma molecules is given by:

$$\bar{v} = (8kT/\pi\mu)^{1/2} \qquad (8)$$

where, k = Boltzmann's constant,

and μ = reduced mass of the colliding particles.

Since we assume that H_2O is the most abundant molecule, the coma can be considered as a mixture of molecules in an H_2O gas, i.e., H_2O is always at least one of the collision partners. The values of the average relative speeds for H_2O collisions with H_2O, CO_2, CO, and NH_3 at T=200 K lie between 0.57 km s^{-1} and 0.73 km s^{-1}. All of these are fairly close to the average outflow velocity of the gas (Delsemme 1982), so we will assume $\bar{v} = v'$. Then, equation (7) simplifies to:

$$D_{\downarrow} = (Q_{H_2O}\sigma_{\downarrow}/4\pi g_{band})^{1/2} \qquad (9)$$

In a similar manner a disequilibrium distance, $D_{\downarrow}$, can be defined as the distance from the nucleus outside of which vibrational radiative relaxation begins to dominate collisional de-excitation. Setting the radiative relaxation rate equal to the collisional relaxation rate yields:

$$D_{\downarrow} = (Q_{H_2O}\sigma_{\downarrow}/4\pi A_{u\ell})^{1/2} \qquad (10)$$

It is important to discuss disequilibrium distances for both excitation and relaxation because it is possible, for example, for collisions to dominate the relaxation of the molecule while being unimportant in its excitation. If this occurs then collisions will quench the potential IR fluorescence.

For rotational transitions, the radiative pumping rates should be very small because both the radiation densities and the transition probabilities are much smaller than their values for electronic and allowed vibrational transitions. In this case, we see from equation (4) that LTE holds only when $A_{u\ell} << C_{u\ell}$. Setting the collisional and radiative relaxation rates equal to each other defines an expression for the rotational disequilibrium distance. This expression can be obtained from equation (10) above by substituting quantities appropriate for pure rotational transitions for the corresponding vibrational quantities.

When collisional effects are unimportant, allowing rotational relaxation, the number of lines in a particular vibrational emission band will be greatly reduced but the brightnesses of the remaining lines will be greatly enhanced. However, fluorescence in vibrational or electronic transitions may result in significant rotational pumping, reducing this enhancement. In the extreme case, the effective rotational temperature could be as high as the color temperature of the sun (this effect has been observed, for example, in C_2). Even when we find that the rotational disequilibrium distance derived using equation (10) is small, we must still assess whether complete rotational relaxation does indeed occur by comparing the Einstein A's for rotational transitions to the g-factors for vibrational and electronic transitions.

III. Individual Molecules

The disequilibrium distance is not very sensitive to the specific value chosen for Q_{H_2O}, as long as a "reasonable" number is used, i.e., the number should be representative of observed comets. Table 1 lists water production rates at R = 1 a.u. for several comets which range from "moderately-bright" to "bright". We choose $Q_{H_2O} = 2X10^{29}$ molecules s^{-1} as an appropriate value.

Collisions having H_2O as a partner are unusually efficient, and even (T-V) cross sections can approach the gas kinetic values. Table 2 lists the collision relaxation cross sections (σ_{V+}) for (T-V) collisions between H_2O and H_2O, CO_2, NH_3, and CO. These values were derived using experimental data from Taylor and Bitterman (1969) and Hirschfelder, Curtiss, and Bird (1964) scaled to the temperature of interest (T = 200 K). Since the experimental data usually covered a fairly wide range of temperatures and extended down to T~300 K, we feel that our extrapolation to 200 K could not be significantly incorrect. For NH_3, we have made the additional assumption that NH_3-H_2O collisions are similar to NH_3-NH_3 collisions. Also, for CO we assume that N_2-H_2O or collisions are indicative of CO-H_2O collisions (according to Taylor and Bitterman 1969, N_2 and CO are expected to behave similarly). The cross sections given refer to the lowest energy vibrational fundamental for each molecule. Collisions relaxing more highly excited vibrational levels must exchange more energy and will generally have smaller cross sections than those listed (However, see the discussion in section II concerning the role of (V-V) collision processes).

Rotational transitions (T-R) are expected to occur for nearly every collision. Experimental data on collisional rotational relaxation are difficult to find and are probably non-existent for the specific interactions considered

here. Generally, those data which do exist indicate cross sections comparable to the gas kinetic values, so we have assumed that the (T-R) cross sections ($\sigma_{\downarrow R}$) are identical with the gas kinetic values. These have been calculated using data from Hirschfelder, Curtiss, annd Bird (1964) and are listed in Table 2.

Radiative pumping rates are required for calculating the disequilibrium distance ($D_{\uparrow}$) for vibrational excitation (eqtn. 9). Chamberlain (1978) defines the "g-factor" to be the fluorescence rate due to scattering of the local solar flux. For a two-level system,

$$g = (\pi e^2/mc^2)\ f\ F_{\odot} \tag{11}$$

where $\pi e^2/mc^2 = 8.82 \times 10^{-13}$ cm,

$f \equiv$ absorption oscillator strength for the transition,

and $F_{\odot} \equiv$ the solar flux at the position of the comet, which is assumed to have R = 1 a.u.
(photons $cm^{-2}\ s^{-1}/cm^{-1}$)

In IR spectroscopy, the "absorption strength" (S_{line}, cm $molecule^{-1}$) is commonly used instead of the oscillator strength (see Penner 1959 or Pugh and Rao 1976). The two quantities are related by:

$$S_{line} = (\pi e^2/mc^2)\ f_{line}\ q \tag{12}$$

where, $q \equiv$ fraction of the total number of molecules which are in the

absorbing level. It is computed in the usual manner from Boltzmann factors and the partition function as described, for example, in Herzberg (1945).

We generalize the above expressions to a vibrational band by writing (the solar flux does not vary appreciably within each vibrational band):

$$g_{band} = F_{\odot} \Sigma S_{line} = F_{\odot} S_{band} \tag{13}$$

The band strengths for H_2O and CO are taken from Rothman (1981), and those for CO_2 are taken from Rothman and Benedict (1978). The band strength for the NH_3 ν_2 transition is taken from Taylor (1973). Solar fluxes are obtained from Labs and Neckel (1968). The band absorption strengths, band g-factors, and the solar fluxes used are given in Table 3 (see also Sec. IV).

Using the collisional cross sections (Table 2) and the band g-factors (Table 3), we calculate (eqtn. 9) vibrational disequilibrium distances for excitation (D_t, Table 4). Radiative excitation will apparently dominate collisional excitation throughout most of the cometary coma. The largest disequilibrium distance is for the ν_2 band of CO_2, but even in this case scattering of solar photons will be the most important excitation mechanism for regions farther than $\sim$400 km from the nucleus.

The radiative transition rate (A_{line}, s^{-1}) for a ro-vibrational transition is given by:

$$A_{line} = (8\pi cd/q)\, \nu^2\, S_{line} \qquad (14)$$

where, $c \equiv$ speed of light in vacuum (cm s^{-1}),

and $d \equiv$ ratio of the statistical weight of the lower state to that of the upper state.

Thus, we define the band Einstein A value (A_{band}, s^{-1}) by:

$$A_{band} = 8\pi cd\nu_{band}^2 S_{band} \qquad (15)$$

where, $\nu_{band} \equiv$ wavenumber for the band origin (cm^{-1}).

The Einstein A's and wavenumbers for all of the vibrational bands considered in this paper are given in Table 4.

Using the Einstein A's (Table 4) and collisional cross sections (Table 2), we calculate (eqtn. 10) vibrational disequilibrium distances for relaxation ($D_\downarrow$, Table 3). Despite the relatively large values for some of the collisional cross sections, all the D's are very small. Apparently, vibrational disequilibrium will occur very close to the surface of the nucleus for all the molecules considered.

Rotational disequilibrium distances for relaxation are calculated using rotational Einstein A's and the cross sections for (T-R) collisions from Table 2. Due to the ν^3 dependence of the Einstein A's, their values can vary over a few orders of magnitude depending upon whether we are referring to low J or high J (J $\equiv$ total angular momentum quantum number) transitions. The A's listed in Table 3 are typical low J values (values for higher J transitions are larger).

We calculate the Einstein A's for NH_3 and CO following Somerville (1977), and we use the values given for H_2O by de Jong (1973). The derived rotational disequilibrium distances are given in Table 4, and their significance is discussed in Section IV.

Disequilibrium distances are not calculated for OH. Since OH is a dissociation product, it is found mainly in the outer coma, where densities are low. Also, vibrational and rotational transitions are electric dipole allowed in OH so that it relaxes rapidly after excitation. For these reasons, collisions are expected to be relatively unimportant for this molecule. This conclusion is apparently supported by the agreement between the theoretical results, derived assuming pure fluorescence equilibrium in OH, and the observations of OH in comets (Schleicher and A'Hearn 1982).

IV. IR Fluorescence

Having shown that collisions cannot maintain vibrational LTE for the molecules considered, we can now calculate their IR fluorescence rates. This process will be the primary source of IR photons from the cometary molecules.

The line-integrated volume emission rate (j) can be expressed as:

$$j = g\, n(r) \quad (\text{photons cm}^{-3}\ \text{s}^{-1}) \tag{16}$$

where, $n(r)$ ≡ the number density of the molecule being considered at the radial distance "r" from the nucleus (cm^{-3}).

Under optically thin conditions, the surface (or column) brightness (B) is given by the integral of the volume emission rate along the line of sight (Chamberlain 1978). Assuming that "g" does not vary with position in the coma:

$$B = 4_{\pi}I = g\,N \qquad (17)$$

where, $B \equiv$ surface brightness (photons $cm^{-2}\ s^{-1}$, usually expressed in Rayleighs where: 1 Rayleigh = 10^6 photons $cm^{-2}\ s^{-1}$),

$I \equiv$ line integrated specific intensity (photons $cm^{-2}\ s^{-1}\ sr^{-1}$),

and $N \equiv$ column density of the molecule in question (cm^{-2}).

Our assumption that "g" does not vary along the line of sight is equivalent to assuming that each volume element in the coma "sees" the same value of solar flux. This means that there is negligible optical depth along the path connecting the sun with the volume element in question. However, for regions very close to the nucleus, large optical depths can be encountered in molecular lines for both the path connecting the given volume element to the sun and for the path connecting this volume element to the observation point. The radiative transfer for the IR fluorescence is thus extremely complicated (Note that proper inclusion of the line shape will further complicate matters because no single velocity distribution is valid for all points in the coma and the local velocity distributions will be neither isotropic nor Maxwellian). The brightnesses calculated using equation (17) will be upper limits. Calculating g-factors as

if optical depth effects could be neglected is instructive for several reasons. First, when the optical depths are not too large the optically thin g-factor may produce reasonably accurate brightness predictions. Second, outflow effects tend to reduce self shielding of the inner coma. Finally, it is interesting to compare the IR g-factors derived here for the cometary parent molecules, to the UV and visible g-factors derived for various dissociation products already observed in comets.

To account for optical depth effects in an approximate way, we also calculate some IR brightnesses using the following model. Consider a sphere centered on the nucleus, whose radius (r_0) is chosen such that the line center optical depth (τ_0) measured along the path from the sun to the nucleus, reaches unity at the surface of the sphere (the column density at which τ_0=1 is calculated assuming a Doppler line profile characterized by a kinetic temperature of 200 K). We assume that the sphere so defined uniformly scatters into 4π steradians all of the solar flux incident upon it at the center frequency of the molecular line. This scattered flux provides the emergent intensity at line center for the cometary emission, which is assumed to have a rectangular profile with a width of 1.6 km s^{-1}. Integrating over the lineshape then gives the amount of radiation scattered by the entire coma in the line being considered. This procedure neglects details of the fluorescence process, but allows an easy calculation of the scattered flux. The physical justification for this model is derived from the fact that scattering of the solar flux becomes significant at $\tau_0 \sim 1$, so that little of the solar flux at line-center will penetrate deeper into the coma. A rectangular line profile crudely approximates the reduction of self-shielding due to outflow. In all cases for which we have made calculations this procedure gives a lower

brightness than the optically thin formalism, indicating that at least we have moved in the right direction (although not necessarily to a more accurate prediction).

The molecular densities needed for making brightness calculations are given by eqtn. (6), replacing the various parameters pertaining to H_2O with those appropriate for the molecule under consideration. Photodestruction lifetimes are given for individual molecules in Table 5. A radial outflow velocity of 0.8 km s^{-1} is used for all molecules (the actual values probably lie between 0.5 and 1 km s^{-1}; see Weaver et al. (1981) and Delsemme (1982)). The column density is obtained by numerical integration of the density distribution along the line of sight. The parameter (r_o) is obtained by integrating the optical depth along the sun-nucleus line, starting at very large values of r (where the density is extremely low due to expansion and lifetime effects) and proceeding to the point where the optical depth equals unity, at line center.

Nearly all observational evidence indicates that H_2O is the most abundant constituent of cometary nuclei, and so we consider its g-factors first. In particular, we consider its ν_3 fundamental band (001-000) at $\lambda \sim 2.66$ μm (3756 cm^{-1}). Fig. 2 is an energy level diagram showing the lowest few rotational energy levels in both the upper and lower vibrational states of this band. The molecular ensemble, and thus the energy diagram, is divided into two non-interacting parts, the ortho form of H_2O having a statistical weight three times that of the para form. Angular momentum quantum numbers and the various symmetries of the levels are indicated in Fig. 2 (see Herzberg (1945) for details). Typical Einstein A's and the electric dipole selection rules governing these transitions are given in de Jong (1973). Certain rotational

levels form a "backbone" (de Jong 1973), defined by the lowest energy levels for a particular value of J (J ≡ total angular momentum quantum number). Using the formalism of sections II and III, we find that cometary H_2O molecules not originally in the backbone levels will very quickly relax to these levels. Furthermore, the backbone levels will quickly relax to the lowest possible value of J. The relaxation rates decrease as J decreases but, as can be seen from Table 4, the rotational populations are expected to relax within ~ 1000 km from the nucleus even for the lowest energy levels. Thus, the conditions in the coma are seen to differ radically from the usual LTE situation. In LTE, many energy levels are populated leading to complex spectra (H_2O is an asymmetric rotor) with numerous lines in each vibrational band. However, in comets we expect to see a large reduction in the number of emission lines and, consequently, a tremendous enhancement in the brightnesses of those remaining in each vibrational band, since all of the band strength will be concentrated into those few lines.

We have calculated g-factors for individual lines in the ν_3 band of H_2O assuming that 25% of H_2O molecules are in the 0_{00} level of the ground state and 75% of the molecules are in the 1_{01} level of the ground state. This is the expected population distribution when all of the H_2O molecules are completely relaxed and assuming that the ortho and para forms of H_2O have a relative abundance equal to the ratio of their statistical weights. Under these conditions, only six transitions are possible in the ν_3 band, and these are indicated in Figure 2. Oscillator strengths and branching ratios were computed from the individual line strengths given in the Air Force Geophysics Laboratory (AFGL) molecular line atlas, using the formalism of Section III. The individual line g-factors are given in Figure 3. The g-factor for the band is given in

Table 3 (see Section III).

Yamamoto (1982) derives a band value which is 1.13 times larger than ours. Since we have not been able to determine exactly how he performed his calculation we cannot account for the difference. However, we consider this difference to be small and conclude that the two calculations for the band g-factor are in agreement. We disagree with Yamamoto (1982) significantly on the predicted shape of the band. Yamamoto (1982) assumes an intensity distribution characteristic of H_2O in LTE at T = 300 K. Our results indicate that the number of H_2O lines in the ν_3 band may be reduced to four very intense lines and two weaker lines. We also note that IR pumping will produce several intense rotational lines in the far infrared (see Figure 2).

Encrenaz et al. (1982) derive a band value which is $\sim$1.2 smaller than ours. Since we use virtually identical values for the IR absorption strengths and solar intensity, the difference apparently arises in the calculations themselves. The intensity distribution within the band is virtually identical in the two cases, reflecting the fact that both groups have independently used similar arguments to justify the population distribution described above.

A component of the cometary nucleus more volatile than H_2O and which is present in substantial amounts ($\sim$10-15% relative to H_2O), is apparently necessary to explain the vaporization behavior of certain new comets. CO_2 and CO have both been proposed as candidates for this volatile component (Delsemme 1982).

Due to its symmetry, the CO_2 molecule does not have a permanent electric

dipole moment and, thus, its rotational levels cannot relax radiatively. In the inner coma, the rotational excitation will be dominated by collisional processes while IR fluorescent pumping will determine the rotational distribution in the outer coma. A detailed model is needed to compute the relative contribution of each component in a given field of view (FOV). We assume here that the intensity distribution within the CO_2 vibrational bands is given by the LTE distribution at T=200 K.

We have calculated g-factors for individual transitions in the ν_3 band of CO_2 ($00^0 1$-$00^0 0$) centered at λ = 4.26 μm (2349 cm^{-1}), and the results are indicated schematically in Figure 3. Each emission line is pumped by two absorptions (P and R), and the pumping rates were calculated after scaling the AFGL line strength data from 296 K to 200 K. Branching ratios into the emission line being considered were derived using eqtn. (14). The ν_3 band of CO_2 is one of the strongest IR bands known, indicating that CO_2 might be detectable in the coma to fairly low abundance levels. The band g-factor is listed in Table 4 and is approximately a factor of ten larger than the H_2O ν_3 band g-factor. Yamamoto (1982) gives a g-factor for the CO_2 ν_3 band which is virtually identical with ours.

The lower rotational levels of CO are maintained in LTE out to fairly large distances from the nucleus (Table 4). Since the Einstein A coefficients for rotational transitions scale as J^3, we would expect the higher energy levels to relax much more quickly. However, time constants for CO are slow enough that a steady state assumption may be invalid (see discussion, section II). A detailed calculation addressing CO excitation in cometary comae is in preparation (Weaver and Chin 1983). Pending completion of the exact model, we will assume that the

population distribution of the rotational levels is given by the LTE value at T = 200 K. The intensity distribution in the g-factors for the (1,0) band of CO (Figure 3) should be considered as illustrative only since the actual intensity distribution could depart significantly from this. The g-factors were calculated in the same manner as described above for CO_2, using molecular data derived from the AFGL compilation. The center of the CO (1,0) band is at λ = 4.67 μm (2143 cm^{-1}). Each emission is pumped by two absorptions (P and R). We emphasize that direct IR pumping in the (1,0) band was the only excitation mechanism retained. This is also true for the polyatomic molecules considered here, but other excitation mechanisms may be particularly important for diatomic molecules (cf. Sec. II). The g-factor derived for the (1,0) band is given in Table 3. Notice that the band g-factor for CO is very close to the value derived earlier for the ν_3 band of H_2O. Yamamoto's (1982) band value for CO is in good agreement with our value, differing by only 10%.

NH_3 is no longer considered to be an abundant constituent of the nucleus, but it has special significance for us because we have an instrument (Mumma et al. 1982) which may provide a sensitive measure of its abundance. NH_3 is a symmetric top molecule which exhibits "inversion doubling" (Herzberg 1945). Figure 4 is an energy level diagram for the ground state of NH_3 and shows the inversion doubling, rotational structure, and the symmetry properties of the ground vibrational state. Following section II (see Table 4), transitions within each "K-ladder" will quickly relax the molecule so that only the J=K levels are populated. The transitions with $\Delta K \neq 0$ are not allowed under electric dipole selection rules, hence the J=K levels are metastable. Since the Einstein A coefficients connecting the inversion doubled levels are very small ($A \sim 2 \times 10^{-7}$ s^{-1}), the antisymmetric and symmetric levels form independent

reservoirs within each J = K level (except for J = K = 0 which possesses only an antisymmetric level). We thus use a partition function for cometary NH_3 in which only the J = K levels of NH_3 are populated, and we take the population distribution among these levels to be characteristic of the temperature in the inner coma, i.e., T = 200 K..

We have calculated g-factors for 122 lines in the ν_2 band of NH_3 located near 10.5 μm (950 cm^{-1}) using molecular data from Taylor (1973). The values for the strong lines are shown in Figure 5. Absolute strengths were calculated using the non-LTE partition function, invoking the sum rule, and normalizing to the vibrational band strength (Taylor (1973)). Selection rules dictate that only Q and R pumping lines are possible. Except when K = 0, a Q absorption pumps both Q and P lines in emission, while an R absorption pumps R, P, and Q emissions. For K = 0, only an R absorption is possible and this pumps only R and P lines in emission. Individual oscillator strengths were calculated using equation (12) and equation (14) was utilized to derive branching ratios. The g-factor for the ν_2 band is listed in Table 3. In contrast to the case of LTE, we see that nearly 10% of the entire band emission is concentrated into a single line, sQ (3,3)! Yamamoto (1982) gives a g-factor which is a factor of 3.3 smaller than our value. We do not know the source of this discrepancy.

Finally, we have calculated g-factors for lines in the (1,0) band of OH centered at λ = 2.80 μm (3570 cm^{-1}). We assume that all OH molecules are in the lowest rotational and vibrational level of the ground electronic state ($^2\pi_{3/2}$). OH is thought to be a photodissociation fragment of H_2O and is found mainly in the outer coma where collisions are not important, allowing complete vibrational and rotational relaxation to occur. We assume that UV fluorescent pumping does

not produce significant equilibrium populations in its excited vibrational or rotational levels. These assumptions are supported by detailed calculations which indicate that even in fluorescence equilibrium over 95% of the OH molecules are in the lowest energy level (cf. Schleicher and A'Hearn (1982)).

Under the conditions described above, there are only two possible absorptions in the (1,0) band and these pump five emission lines (here a line is defined as a sum over both Λ-doubled components; see Schleicher and A'Hearn (1982) for a description of the ground electronic state of OH). Unlike our previous calculations we also include the contribution to the (1,0) band emission by pumping in the (2,0) band followed by cascade in the (2,1) band. The contribution to the (1,0) band g-factors from this excitation mechanism is generally about 10-20% of the contribution from direct pumping in the (1,0) band. There are two absorptions possible in the (2,0) band and these pump the same five emission lines mentioned above plus three more lines (however, since these latter three lines are pumped only by absorption in the (2,0) band their g-factors are smaller than the others). Einstein A coefficients for the allowed transitions are taken from Mies (1976). Although recent work (Goldman 1982) suggests that the A's for the (1,0) band transitions should be reduced by a factor of 0.58, we will use the Mies values until this matter has been resolved conclusively. We simply note here that reducing all of the (1,0) band Einstein A's by a common factor will reduce the g-factor by approximately this same amount. The Einstein A's are used to calculate oscillator strengths using eqtns. (12) and (14). The solar flux used for the (2,0) band is 4.7×10^{13} photons cm^{-2} s^{-1}/cm^{-1} (Labs and Neckel 1968). Using these data, we have calculated g-factors for all the possible emission lines and these are shown in Figure 5a. The g-factor for the (1,0) band is given in Table 3. The value

derived by Yamamoto (1982) is a factor of 1.8 larger than ours. Since we do not know the details of his calculation we cannot account for this difference.

The fluorescence model of Schleicher and A'Hearn (1982) predicts directly the populations of the relevant rotational and vibrational levels of the ground state of OH. An individual line g-factor can be obtained from their results by multiplying the relative upper-state population by the Einstein A for that transition. The band g-factor derived from their data is a factor of ~2 smaller than our value (Table 3), and although it depends weakly on heliocentric velocity (through the UV pumping rate) this does not explain the discrepancy. Since we included only IR pumping in the (1,0) and (2,0) bands as excitation mechanisms, our calculation should yield a lower limit for the g-factors. Schleicher and A'Hearn (1982) neglected IR pumping mechanisms, and the IR band g-factors based on their model will give only the contribution made by UV excitation. By examining the relevant excitation and decay rates it is clear that direct IR pumping is about a factor of two stronger as an excitation source for IR emissions than is UV pumping. Schleicher and A'Hearn (private communication) have recently confirmed this by including IR pumping in both the (1,0) and (2,0) bands in their model. Their results for R = 1 a.u. and $\dot{R}$ (≡ heliocentric radial velocity) = 0 km s^{-1} are shown in Fig. 5b. UV fluorescence causes population leakage from the $^2\pi_{3/2}$ to the $^2\pi_{1/2}$ levels and, therefore, they predict the presence of twice as many lines as our calculation. Their new value for the (1,0) band g-factor is a factor of 1.5 larger than ours, of which 2/3 represents direct IR pumping and 1/3 represents UV pumping. We note that the UV pumping of the IR (1,0) band represents an example of "Franck-Condon pumping", mentioned earlier (section II) as a potentially important excitation mechanism for diatomic molecules. Even in OH, which has a relatively narrow

Franck-Condon envelope with relatively little vibrational pumping, the Franck-Condon pump contributes one third of the total IR excitation.

V. Discussion

We have demonstrated that vibrational LTE cannot be maintained in the coma, except possibly within a very small region around the nucleus, and that scattering of solar photons in fundamental ro-vibrational transitions of cometary parent molecules is expected to be the primary source of IR molecular emissions from comets. Moreover, these IR excitation rates are rather large (Table 3). The g-factor for the ν_3 band of CO_2 exceeds the value of some of the strongest observed UV transitions (for example, the g-factor for the OH (0,0) band at λ = 3090 Å varies between 2 X 10^{-4} and 10 X 10^{-4} photons s^{-1} $molecule^{-1}$, depending on the heliocentric velocity). However, IR detectors are generally much less sensitive than UV or visible detectors (which can operate at the photon-counting limit), and large g-factors alone are no guarantee that the emissions are large enough to detect. The strengths of the IR molecular emissions from a typical moderately bright comet must be compared to the sensitivity limits of presently available IR instrumentation.

We have chosen to predict the IR molecular emission from comet Bradfield (1979 X), a moderately-bright comet that was well-characterized by UV observations made with the International Ultraviolet Explorer satellite observatory in early 1980 (Feldman et al. 1980, Weaver et al. 1981). The observational parameters (R,Δ) are listed in Table 6, and are appropriate for comet Bradfield (1979 X) on 10 January 1980. The bright comet Bennett (1970 II) was observed by Ney (1974) in the IR (using filter photometry) under similar

observational conditions during 1970.

Molecular production rates are given for comet Bradfield (1979X) in Table 6. OH production rates were derived from measurements of its (0,0) band emission which was the brightest feature in the UV spectra (Weaver et al. 1981). Assuming that ~90% of the H_2O molecules dissociate into OH molecules and H atoms, Weaver et al. (1981) found $Q_{H_2O} = 2 \times 10^{29}$ molecules s^{-1} for $v_{H_2O} = 1$ km s^{-1}. Since we use $v_{H_2O} = 0.8$ km s^{-1}, we scale the production rate appropriately. The CO_2 production rate is obtained from measurements of the CO_2^+ ion (Festou, Feldman, and Weaver 1981) and is approximately 10% of the H_2O production rate. It is not yet clear which of CO_2 or CO is more abundant in comets. Feldman and Brune (1976) measured a CO production rate which was ~0.3 of the H_2O production rate for comet West (1976 VI). CO was tentatively identified in comet Bradfield (1979 X) (A'Hearn and Feldman 1980) and appears to be approximately five times less abundant than CO_2 in this comet. We choose the CO production rate to be identical to that of CO_2. The NH_3 production rate is the most uncertain quantity. Based on measurements of NH_2 in some comets, A'Hearn (1982) estimates the production rate of this molecule to be $\gtrsim$ 0.1% of the H_2O production rate. Since NH_2 is thought to be a primary photodestruction product of NH_3 (Huebner and Carpenter 1979), NH_3 is expected to have a production rate similar to NH_2. However, due to the uncertainties involved we have decided to use $Q_{NH_3} = 0.1\ H_2O$. Of course, if NH_3 is not in the nucleus then it will never be observed.

The average column density was calculated for each species within a 10" X 15" field of view (FOV), the effective aperture for the IUE observations. These are listed in Table 6. An outflow velocity of 0.8 km s^{-1} was used for all molecules except OH. The OH outflow velocity was assumed to be 1.15 km s^{-1}

(Weaver et al. 1981). The average surface brightnesses in the FOV were obtained using eqtn. (17) after scaling the g-factors (Table 3 and Figures 3, 5 and 6) to R = 0.71 a.u. using an inverse square law. We have listed the intensities in Table 6 using two systems of units: (1) Watts cm^{-2} sr^{-1}, which is common in IR astronomy, and (2) Rayleighs, which is commonly used in UV and visible astronomy. The flux at the earth can be obtained from the intensity by multiplying by the solid angle of the FOV (3.5×10^{-9} sr, for our example).

The predicted IR emissions are comparable to the brightest observed UV emissions. For example, the OH (0,0) band of comet Bradfield (1979 X) had a brightness of 370 kR, while the H Lyα line brightness was 160 kR. Furthermore, we emphasize that the brightnesses of the IR emissions are not always distributed among many lines. There should be a tremendous reduction in the number of lines relative to the LTE case for H_2O, OH, and NH_3 emissions. Thus, high spectral resolution instruments may have an advantage in the detection of these lines (we will elaborate on this later).

The sensitivity of a presently available Fourier Transform Spectrometer (FTS), similar to the one used by Johnson, Fink, and Larson (1983) for their observations of comet West (1976 VI), is approximately 1.2×10^{-12} Watts cm^{-2} sr^{-1} (this corresponds to $\sim$210 Rayleighs near λ = 2.7 μm) in the region of the H_2O and OH bands (Larson, private communication). This sensitivity limit has been calculated assuming detector noise limited operation of the instrument, a spectral resolution of 4 cm^{-1} (this is the same resolution used for the comet West (1976 VI) observations), a telescope aperture of 1.8×10^4 cm^2, and an integration time of one hour. The FOV of their instrument is similar to the value discussed above (depending on what detector they use, the FOV is either

20" X 20" or 10" X 10"), but for our calculation we assume their FOV is exactly 10" X 15". Comparing with Fig. 2, we see that at 4 cm^{-1} resolution individual lines of the ν_3 band of H_2O are completely resolved, while there will be $\sim$3-4 lines of the ν_3 band of CO_2 in each resolution element (let us assume for the moment that the FTS is as sensitive near 4.3 μm as it is near 2.7 μm, and that detector-noise limited operation is also possible at 4.3 μm). In Table 7 we give the average intensity in a single resolution element expected from the strongest H_2O line in the ν_3 band and from the sum of the three strongest CO_2 lines in the P-branch of the CO_2 ν_3 band. The expected signal to noise ratios are also given. These intensities appear to be easily detectable.

The average optical depth in the FOV is estimated to be $\sim$0.6 for the H_2O line and $\sim$0.4 for the CO_2 lines. While these average optical depths are not very large we must recognize that since the density distribution peaks very strongly towards the nucleus, radiative trapping and other optical depth effects may play a significant role in the inner coma. Optical depth effects are included approximately by calculating the average intensities using the model described in section III. These values are also listed in Table 7. While they are considerably smaller than the values derived assuming negligible optical depth, these intensities are still above the detector-noise limit of the FTS considered here.

The specific intensity of the molecular lines can greatly exceed the grain emission. Using an empirical formula derived from the observational data on comet Kohoutek (1973 XII) collected by Ney (1974), we have derived the average IR grain brightness in three wavelength regions for a "standard" comet at R = 0.71 a.u. and Δ = 0.62 a.u. (see Table 8). The bandpass was chosen as 4 cm^{-1}.

The values measured for comet Bennett (1970 II) (R = 0.64 a.u., Δ = 0.76 a.u.) were scaled to a FOV of 10" X 15" using the scaling law suggested by Ney (1974) (Table 8). The average specific intensity (Watts cm^{-2} sr^{-1}/cm^{-1}) of the thermal grain radiation is compared with the line-center intensity of the strongest emission line for each molecule in Figure 7. If the IR molecular emissions are as large as predicted, then they should be easily seen in emission against the thermal continuum, using a sufficiently high spectral resolution instrument.

Noise contributed by background thermal radiation from the sky, the telescope, or the instrument itself, may limit the detectability of these cometary lines by ground-based instruments. Since the background consists of greybody radiation at a temperature of $\sim$270-300 K, it will be particularly troublesome in the vicinity of 10 μm. However, even for wavelengths as short as $\lambda \sim 3$ μm, FTS instrument sensitivities may be limited by fluctuations in the sky brightness. Sky noise is difficult to predict theoretically and is highly dependent upon observing conditions (e.g., humidity, beam throw, etc.) and the particular instrument used. Background noise may be greatly reduced by severely restricting the bandpass of the instrument. For cryogenically-cooled space-borne instruments, photon noise from the cometary grain radiation may become important for low spectral resolution instruments (see Yamamoto, 1982).

Telluric absorption is a particularly acute problem for ground-based observations because some of the molecules we are trying to detect in comets are also strong absorbers in the earth's atmosphere (e.g., H_2O, CO_2, and CO). The terrestrial absorption is not as severe for CO (Delbouille et al. 1981) and it may be possible to detect strong CO emissions from a comet whose emission is sufficiently Doppler-shifted away from the terrestrial absorption peak (the

shift should probably be at least 0.3 cm^{-1} corresponding to $\mathcal{Q}$ = 42 km s^{-1}). However, there appears to be little hope for ground-based detections of emissions from H_2O, CO_2, or the OH(1,0) band in the near IR. Detections of CO_2 will probably only be accomplished from space, but it may be possible to detect H_2O and OH IR emissions from comets using instruments at airplane altitudes. For example, the Kuiper Airborne Observatory (KAO) typically cruises at an altitude of 12 km, which is above 99% of the terrestrial wapor vapor.

Finally, we note that the high spectral resolution techniques ($\lambda/\Delta\lambda \gtrsim 10^6$) of laser heterodyne spectroscopy might provide a relatively sensitive measurement of the NH_3 abundance in comets. We calculate that our instrument (Mumma et al. 1982) would be able to detect an NH_3 production rate of $\sim 3 \times 10^{27}$ molecules s^{-1} for a comet at R = 0.71 a.u. and Δ = 0.62 a.u. (The heterodyne instrument has a diffraction-limited FOV which corresponds to $\sim$3" on a 60-inch telescope). The laser heterodyne receiver is also sensitive to the "hot" bands of CO_2 near 10 μm, as well as a host of emissions from other polyatomic molecules (although many of these have never been proposed as constituents of cometary nuclei). In fact, this method may be the only way in which a cometary parent molecule can be detected from the ground in the IR.

VI. Conclusion

It has been demonstrated that the physical conditions in the inner coma of a comet depart rather drastically from LTE. As a result, IR fluorescence of cometary parent molecules is expected to be a strong source of molecular line emissions. These emissions are predicted to be easily detectable using available instrumental sensitivities. However, due mainly to terrestrial

atmospheric absorption, the detection of IR molecular emissions will be a difficult experimental task and may require observations from airborne or space-borne platforms. Since detection of their IR molecular line emissions provides one of the few means by which cometary parent molecules can be identified directly (radio observations being the only other method which comes to mind), further research into this problem should be vigorously pursued.

We acknowledge Dr. J. Bergstralh for deriving the empirical formula for the thermal grain radiation from a "standard" comet.

Table 1

Water Production in Comets

Comet	Water Production Rate (molecules s^{-1})[a]
Bennett (1970 II)	2×10^{29}
West (1976 VI)	4×10^{29}
Bradfield (1979 X)	6×10^{28}

[a]All values are derived from data presented in Festou et al. (1982) and are valid at R (≡ heliocentric distance) = 1 a.u.

Table 2

Data for Collisions of H_2O with Various Molecules[a]

Molecule	$\sigma_{V\downarrow}(cm^2)$[b]	$\sigma_{R\downarrow}(cm^2)$
H_2O	1.5×10^{-15} (ν_2)	2.5×10^{-15}
CO_2	3.5×10^{-16} (ν_2)	3.6×10^{-15}
CO	2×10^{-20} (1,0)	3.2×10^{-15}
NH_3	8×10^{-19} (ν_2)	3.1×10^{-15}

[a]Explanation of symbols and source of these data can be found in section III of the text. $\sigma_{\uparrow}$ may be calculated from $\sigma_{\downarrow}$ by invoking detailed balancing (see Sec. II, eqtn. 4).

[b]The vibrational transition for the (T-V) process considered is listed in parentheses.

Table 3

IR Molecular Emissions: g-Factors

Molecule	Transition	Band Origin (cm^{-1})	Band Strength (cm molecule^{-1})	Solar Flux (photons cm^{-2} s^{-1}/cm^{-1})	[a]Band g-factor (photons s^{-1} molecule^{-1})
H_2O	ν_2	1595	1.0×10^{-17}	2.0×10^{13}	2.0×10^{-4}
H_2O	ν_3	3756	6.9×10^{-18}	3.9×10^{13}	2.7×10^{-4}
CO_2	ν_2	667	8.3×10^{-18}	8.6×10^{12}	7.1×10^{-5}
CO_2	ν_3	2349	9.6×10^{-17}	2.8×10^{13}	2.7×10^{-3}
CO	(1,0)	2143	9.8×10^{-18}	2.5×10^{13}	2.5×10^{-4}
NH_3	ν_2	932,968	2.2×10^{-17}	1.2×10^{13}	2.6×10^{-4}
OH	(1,0)	3570	1.9×10^{-18}	3.8×10^{13}	7.4×10^{-5}

[a]All values are valid for a heliocentric distance of 1 a.u.

Table 4

Disequilibrium Distances[a]

Molecule: Transition	μ_D (Debye)	ν (cm^{-1})	A (s^{-1})	$D_\uparrow$ (km)	$D_\downarrow$ (km)
H_2O: ν_2	1.88	1595	20	11	11
ν_3		3756	74	-	-
rotation		-	4×10^{-3}	-	1000
CO_2: ν_2	0	667	1.4	360	20
ν_3		2349	399	-	-
rotation		-	0	-	∞
CO: (1,0)	0.11	2143	34	0.005	0.03
rotation		-	8×10^{-8}	-	7.7×10^{4}
NH_3: ν_2	1.47	932,968	15	2.3	0.3
rotation					
$J \neq K$, $\Delta J=1, \Delta K=0$		-	1×10^{-2}	-	220
$J = K$, a↔s		-	2×10^{-7}	-	4.9×10^{4}
$J = K$, $\Delta J=1=\Delta K$		-	0	-	∞

[a]Disequilibrium distances are listed in the last two columns. μ_D is the permanent electric dipole moment. Other parameters are defined in section III of the text.

Table 5

Photodestruction Lifetimes

Molecule	Lifetime (τ,s)
H_2O	8.3×10^4
CO_2	5.0×10^5
CO	1.5×10^6
NH_3	5.6×10^3
OH	6.3×10^4

[a]All values are valid at R ($\equiv$ heliocentric distance) = 1 a.u. Reference is Huebner and Carpenter (1979), except for OH which is discussed in Weaver et al. (1981).

Table 6

IR Molecular Emission from a Moderately Bright Comet at R = 0.71 a.u. and Δ = 0.62 a.u.

Molecule	Production Rate(mol s^{-1})	Column[a] Density (cm^{-2})	Transition	Surface Brightness[a] W cm^{-2} sr^{-1}	Rayleighs
H_2O	1.8×10^{29}	3.2×10^{15}	ν_3	1.0×10^{-8}	1.7×10^{6}
CO_2	1.8×10^{28}	3.5×10^{14}	ν_3	7.0×10^{-9}	1.9×10^{6}
CO	1.8×10^{28}	3.6×10^{14}	(1,0)	6.0×10^{-10}	1.8×10^{5}
NH_3	1.8×10^{28}	1.3×10^{14}	ν_2	1.0×10^{-10}	6.7×10^{4}
OH	1.7×10^{29}	2.1×10^{14}	(1,0)	1.7×10^{-10}	3.1×10^{4}

[a]Both the column density and the brightness are average values in a 10" X 15" aperture.

Table 7

Detection Capability for IR Molecular Emissions[a]

Molecule	Transition	Intensity (W cm^{-2} sr^{-1}) Optically thin	S/N	Optically thick	S/N
H_2O	ν_3 band: $0_{oo} - 1_{o1}$	2.7×10^{-9}	2250	2.3×10^{-10}	192
CO_2	ν_3 band: P(12)+P(14)+P(16)	9.5×10^{-10}	792	6.6×10^{-11}	55

[a]Assumptions are stated in the text (section V). Observational conditions are identical to those of comet Bradfield (1979 X) on 10 January 1980. Instrument sensitivities are those of the FTS described by H. P. Larson (private communication). The resolution was chosen to be 4 cm^{-1}. Detector-noise limited operation is assumed in the calculation of all signal-to-noise ratios (S/N).

Table 8

IR Background Radiation: Continuum Radiation from Cometary Grains

	Brightness ($W\ cm^{-2}\ sr^{-1}$)[a]		
	3759 cm^{-1}	2347 cm^{-1}	1000 cm^{-1}
"standard" comet at R=0.71 a.u. and Δ=0.62 a.u.	1.7×10^{-11}	7.4×10^{-10}	8.1×10^{-9}
comet Bennett (1970 II) at R=0.64 a.u. and Δ=0.76 a.u.	1.7×10^{-9}	8.0×10^{-9}	7.0×10^{-8}

[a]These are average intensities in a 10" X 15" aperture. The values are integrals over a spectral interval of 4 cm^{-1}. See section V of the text for further details.

References

A'Hearn, M. F., and Feldman, P. D. 1980, Ap. J. (Letters), 242, L187.

A'Hearn, M. F. 1982, in "Comets", L. L. Wilkening ed., Univ. of Az. Press, Tucson, Arizona, p. 433.

Arpigny, C. 1964, Ann. D'Ap., 27, 393.

Biermann, L., Giguere, P. T., and Huebner, W. F. 1982, Astr. Ap., 108, 221.

Biraud, F., Bourgois, G., Crovisier, J., Fillet, R., Gerard, E., and Kazès, I. 1974, Astr. Ap., 34, 163.

Campins, H., and Hanner, M. S. 1982, in "Comets", L. L. Wilkening ed., Univ. of Az. Press, Tucson, Arizona, p. 341.

Chamberlain, J. 1978, "Theory of Planetary Atmospheres: An Introduction to their Physics and Chemistry", Academic Press, NY.

Crovisier, J. 1982, in proceedings of the ESO Workshop on "The Need for Coordinated Ground-based Observations of Halley's Comet."

deJong, T. 1973, Astr. Ap., 26, 297.

Delbouille, L., Roland, G., Brault, J., and Testerman, L. 1981, "Preliminary

Photometric Atlas of the Solar Spectrum from 1850 to 10,000 cm^{-1}", private communication.

Delsemme, A. H. 1982, in "Comets", L. L. Wilkening ed., Univ. of Az. Press, Tucson, Arizona, p. 85.

Deming, D., and Mumma, M. J. 1983, Icarus, in press.

Despois, D., Gerard, E., Crovisier, J., and Kazes, I. 1981, Astr. Ap., 99, 320.

Dickinson, R. E. 1972, J. Atmos. Sci., 19, 1531.

_____. 1976, J. Atmos. Sci., 33, 290.

Donn, B., and Cody, R. J. 1978, Icarus, 34, 436.

Dossin, F., Fehrenbach, C., Haser, L., and Swings, P. 1961, Ann. D'Ap. 24, 519.

Encrenaz, Th., Crovisier, J., Combes, M., and Crifo, J. F. 1982, Icarus, 51. 660.

Feldman, P. D., and Brune, W. H. 1976, Ap. J. (Letters), 209, L45.

Feldman, P. D., et al. 1980, Nature, 286, 132.

Feldman, P. D., 1982, in "Comets", L. L. Wilkening ed., Univ. of Az. Press, Tucson, Arizona, p. 461.

Festou, M. C. 1981, Astr. Ap., 95, 69.

Festou, M. C., Feldman, P. D., and Weaver, H. A. 1982, Ap. J., 256, 331.

Festou, M. C., Feldman, P. D., Weaver, H. A., and Keller, H. U. 1982, in "Advances in Ultraviolet Astronomy: Four Years of IUE Research", European Conference Proceedings.

Giguere, P. T., and Huebner, W. F. 1978, Ap. J. 223, 638.

Goldman, A. 1982, Appl. Opt., 21, 2100.

Haser, L. 1966, Cong. Coll. Univ. Liège, 37, 233.

Herzberg, G. 1945, "Molecular Spectra and Molecular Structure. II. Infrared and Raman Spectra of Polyatomic Molecules", D. Van Nostrand Co. Inc., N.Y.

Hirschfelder, J. O., Curtiss, C. F., and Bird, R. B. 1964, "Molecular Theory of Gases and Liquids", Second Ed., John Wiley and Sons, N.Y.

Huebner, W. F., and Carpenter, C. W. 1979, "Solar Photo Rate Coefficients", Los Alamos Sci. Lab. Report (LA-8085-MS).

Huebner, W. F., and Giguere, P. T. 1980, Ap. J., 238, 753.

Hunaerts, J. 1953, Mem. Soc. Roy. Sci. Liège, 13, 99.

Johnson, J. R., Fink, U., and Larson, H. P. 1983, Ap. J, in press.

Labs, D., and Neckel, H. 1968, Zs. Ap., 69, 1.

Lane, A. L., Stockton, A. N., and Mies, F. H. 1974, in "Comet Kohoutek", G. A. Gary ed. (NASA SP-355), p. 87.

Malaise, D. J. 1970, Astro. Ap., 5, 209.

Marconi, M. L., and Mendis, D. A. 1982, Ap. J. 260, 386.

Mies, F. H. 1974a, Ap.J. (Letters), 191, 145.

_____. 1974b, J. Mol. Spect., 53, 150.

Mitchell, G. F., Prasad, S. S., and Huntress, W. T. 1981, Ap. J., 244, 1087.

Mumma, M. J. 1980, in "Vibrational-Rotational Spectroscopy for Planetary Atmospheres" (NASA CP-2223), 717.

Mumma, M. J., Kostiuk, T., Buhl, D., Chin, G., and Zipoy, D. 1982, Opt. Eng., 21, 313.

Ney, E. P. 1974, Icarus, 23, 551.

Ney, E. P. 1982, in "Comets", L. L. Wilkening ed., Univ. of Az. Press, Tucson, Arizona, p. 323.

Nuth, J. A., and Donn, B. 1981, Ap.J. 247, 925.

Oppenheimer, M., and Downey, C. J. 1980, Ap. J. (Letters), 241, 123.

Penner, S. S. 1959, "Quantitative Molecular Spectroscopy and Gas Emissivities", Addison-Wesley, Reading, Mass.

Pugh, L. A., and Rao, K. N. 1976, in "Molecular Spectroscopy: Modern Research", Vol. II, N. Rao ed., Academic Press, N.Y., p. 165.

Rothman, L. S., and Benedict, W. S. 1978, Appl. Opt., 17, 2605.

Rothman, L. S. 1981, Appl. Opt., 20, 791.

Schleicher, D. G., and A'Hearn, M. F. 1982, Ap. J., 258, 864.

Shimizu, M. 1976, Ap. Space Sci., 40, 149.

Somerville, W. B. 1977, in "Advances in Atomic and Molecular Physics", Vol. 13, D. R. Bates ed., Academic Press, NY.

Swift, M. B., and Mitchell, G. F. 1981, Icarus, 47, 412.

Taylor, F. W. 1973, JQSRT, 13, 1181.

Taylor, R. L., and Bitterman, S. 1969, Rev. Mod. Phys., 41, 26.

Weaver, H. A., Feldman, P. D., Festou, M. C., and A'Hearn, M. F. 1981, Ap. J. 251, 809.

Weissman, P. R., and Kieffer, H. H. 1981, Icarus, 47, 302.

Whipple, F. L. 1950, Ap. J., 111, 375.

_____. 1951, Ap.J., 113, 464.

Yamamoto, T. 1982, Astr. Ap., 109, 326.

Yamashita, I. 1975, J. Phys. Soc. Japan, 39, 205.

Figure Captions

Figure 1. The flux from comet Bennet (1970 II), derived from the data of Ney (1974). The dotted curve has the shape of a blackbody spectrum at 518 K, which is the temperature most nearly describing the grains, according to Ney (1974). The excess cometary flux at ~10 μm and ~18 μm are described as "silicate features" by Ney (1974). The cometary flux also shows an excess at the shorter wavelengths ($\lambda \lesssim 2.5$ μm) due to scattering of the solar flux by the grains. The solar flux shown is the average continuum flux at 1 a.u. from the sun as derived from the data of Labs and Neckel (1968). The positions of the IR molecular emissions considered in this paper are indicated by arrows.

Figure 2. Diagram showing the lowest energy levels of the (000) and (001) states of the H_2O molecule. The right hand side shows "ortho" levels which have a statistical weight three times that of the "para" levels located on the left hand side. The ortho and para levels are non-interacting. The energy levels are identified by $J_{K_a K_c}$, where J is the total angular momentum quantum number and K_a, K_c are projections of J in the prolate and oblate symmetric top approximations, respectively. Other symmetry properties are indicated in the figure (see Herzberg (1945) for further explanation). The dashed lines show some of the rotational transitions in the ground state which will tend to relax the molecules to the lowest energy levels, as discussed in the text. For

completely relaxed H_2O molecules only the transitions marked with solid lines are important.

Figure 3. G-factors for individual lines in the ν_3 band of H_2O, the ν_3 band of CO_2, and the (1,0) band of CO. The values of the g-factors in absolute units (photons s^{-1} $molecule^{-1}$) are shown for a heliocentric distance of 1 a.u. Also given are the band g-factors, defined as the sum of g-factors over all lines in the band.

Figure 4. Diagram showing the lowest energy levels of the ground vibrational state of NH_3. Except for the K=0 levels, inversion doubling causes a splitting into symmetric (s) and antisymmetric (a) levels. This splitting ($\sim$ 0.8 cm^{-1}) is exaggerated in the figure for illustrative purposes. Total angular momentum quantum number, J, is given next to each level. K is the projection of J along the symmetry axis and its value is indicated along the horizontal axis. Positive and negative signs indicate the parity of the states. See Herzberg (1945) for further details. Electric dipole allowed transitions which relax the NH_3 molecules to the J=K levels (as described in the text) are indicated in the figure.

Figure 5. G-factors for individual lines in the ν_2 band of NH_3. The strongest transitions are identified by quantum number assignments. The values of the g-factors in absolute units (photons s^{-1} $molecule^{-1}$) are shown for a heliocentric distance of 1 a.u. The band g-factor is also given. The P, Q, and R branches are shown separately and different wavenumber scales are used for the aQ and sQ branches.

Figure 6. G-factors for the (1,0) band of OH. (a) shows our calculation which includes only IR pumping. (b) gives the results of Schleicher and A'Hearn (private communication) including both IR and UV pumping. Individual line g-factors and their sum (the band g-factor) are shown for a heliocentric distance of 1 a.u.

Figure 7. The intensity of the thermal radiation from the grains of a "standard" comet is indicated by the curve. The intensities at line center for the strongest lines in the bands considered in this paper are shown as "X". The heliocentric distance of the comet is 0.71 a.u., the geocentric distance is 0.62 a.u., and all intensities are average values in a 10" X 15" aperture. Our model predicts that at the position of the spectral lines, the flux collected from the IR molecular emissions will far exceed that of the grains in a sufficiently high resolution instrument.

M. J. MUMMA and H. A. WEAVER, NASA/Goddard Space Flight Center, Infrared and Radio Astronomy Branch, Laboratory for Extraterrestrial Physics, Greenbelt, MD 20771.

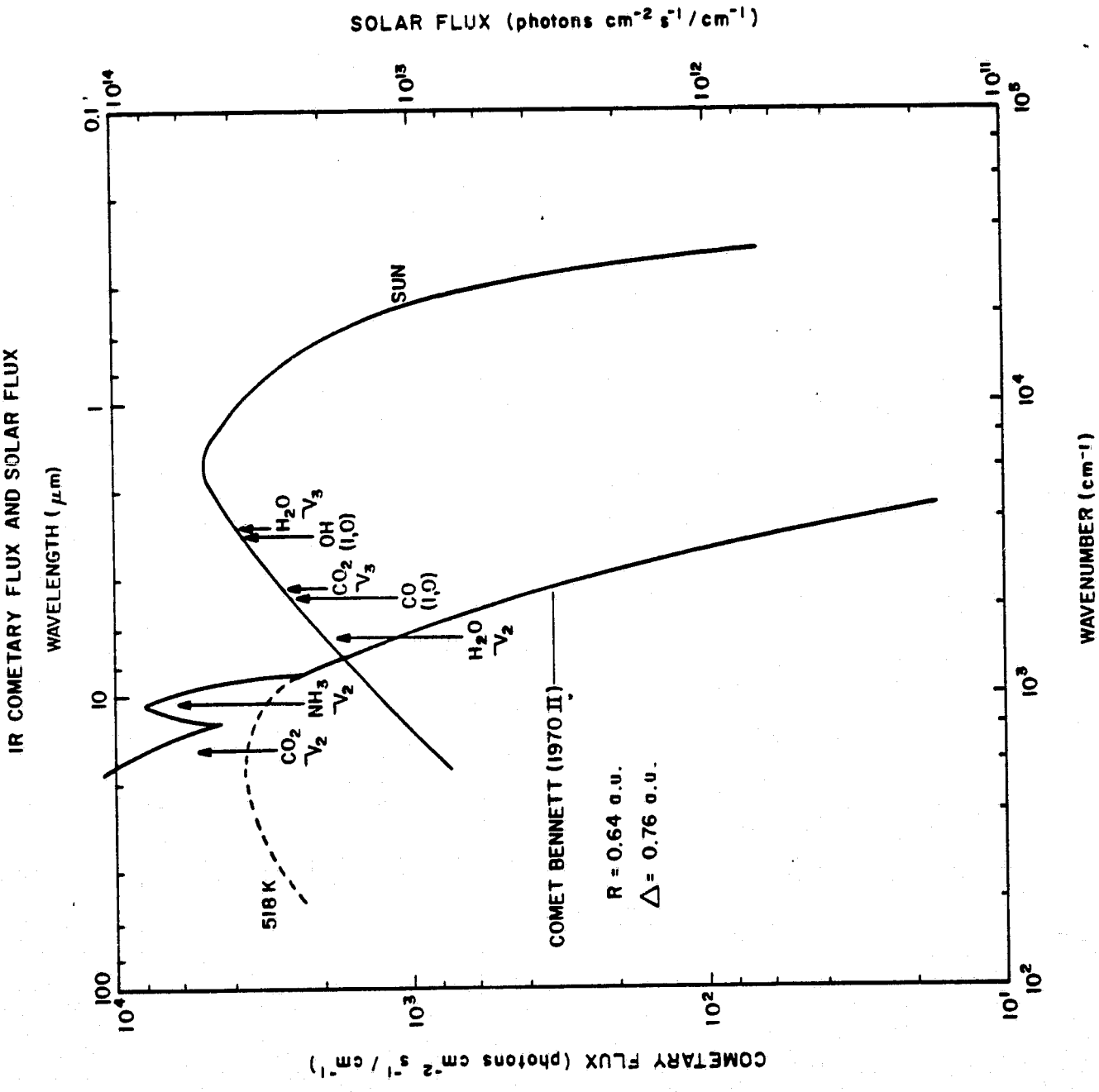

Figure 1

ORIGINAL PAGE IS
OF POOR QUALITY

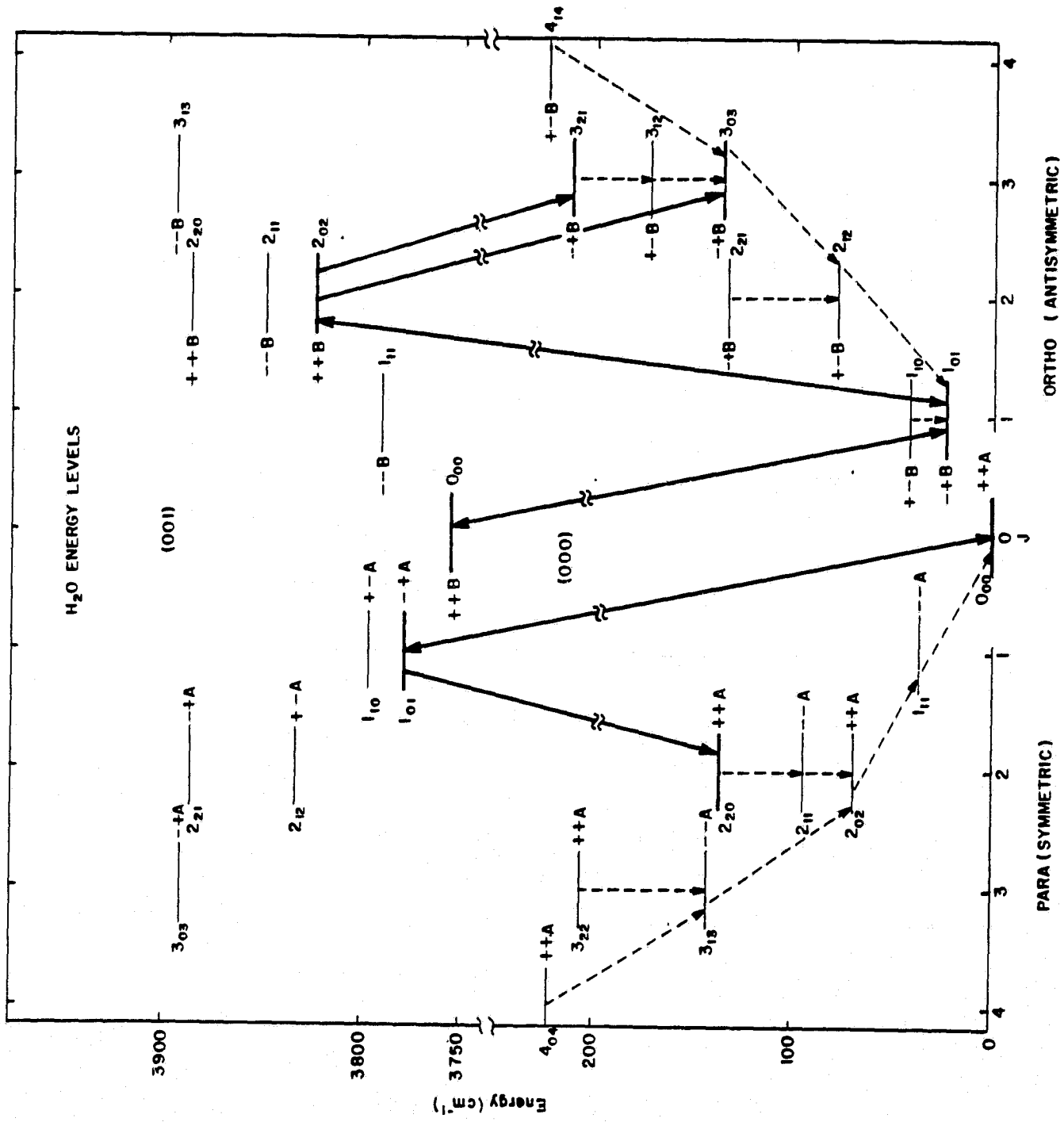

Figure 2

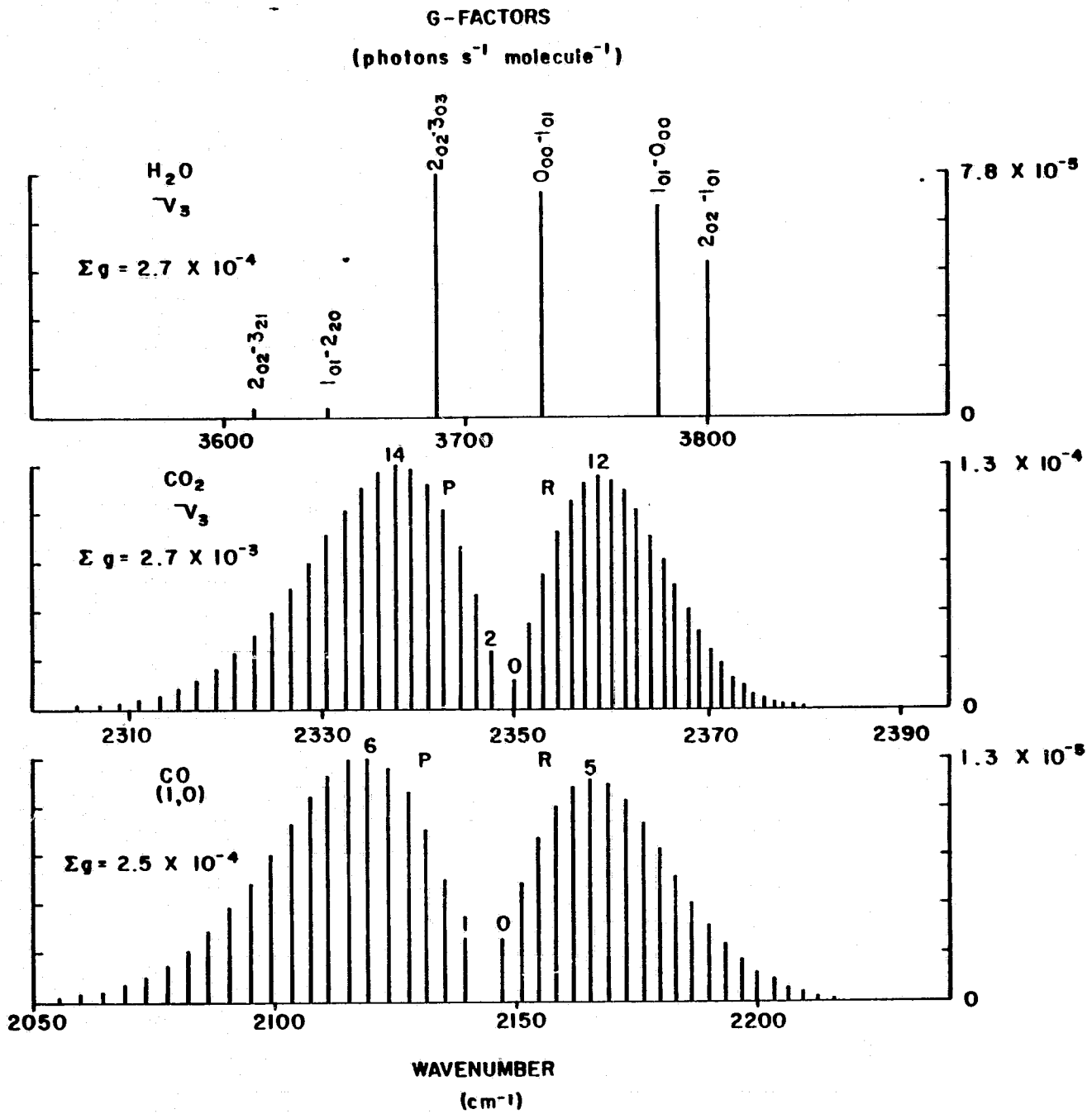

ORIGINAL PAGE IS
OF POOR QUALITY

Figure 3

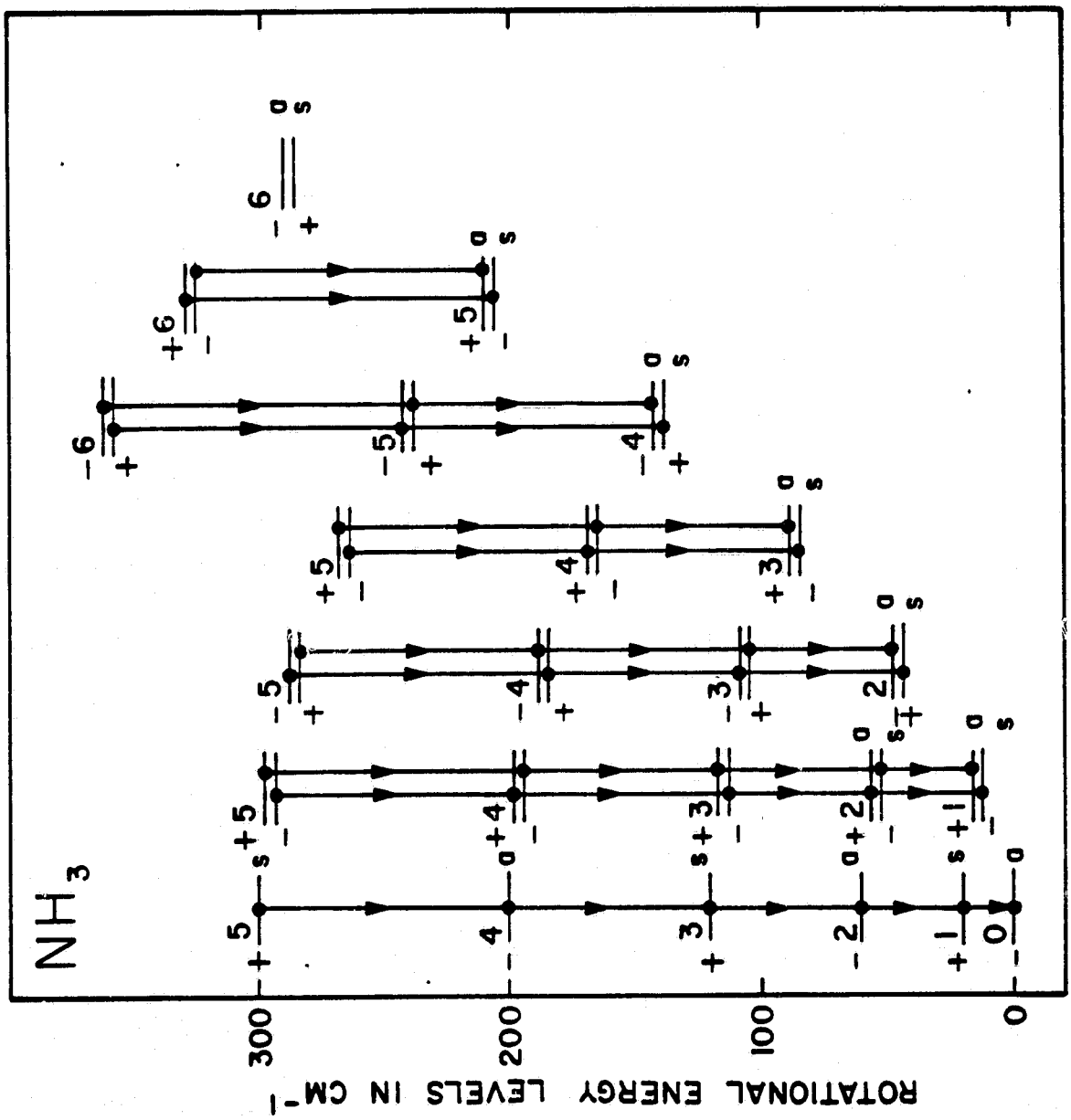

Figure 4

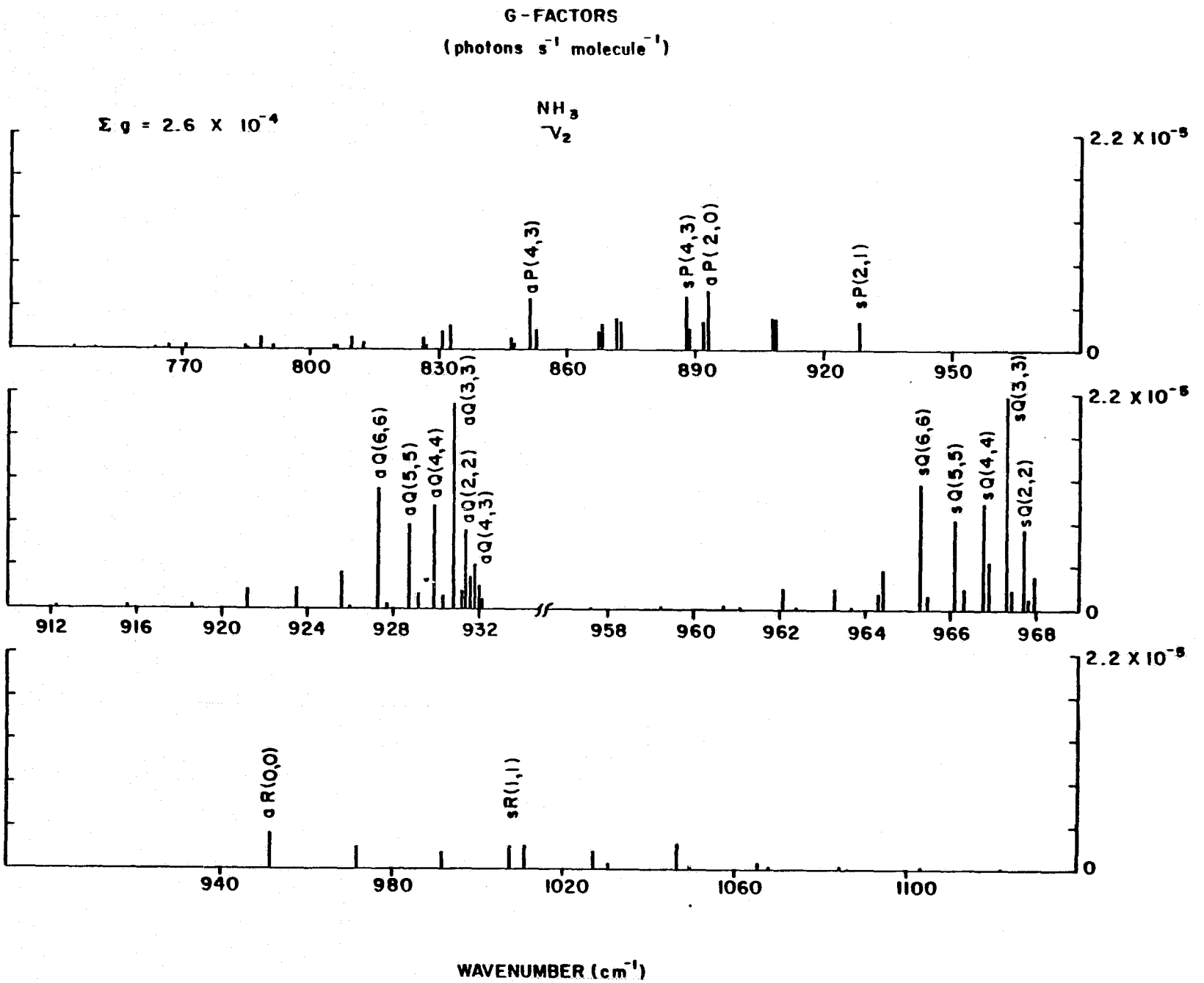

Figure 5

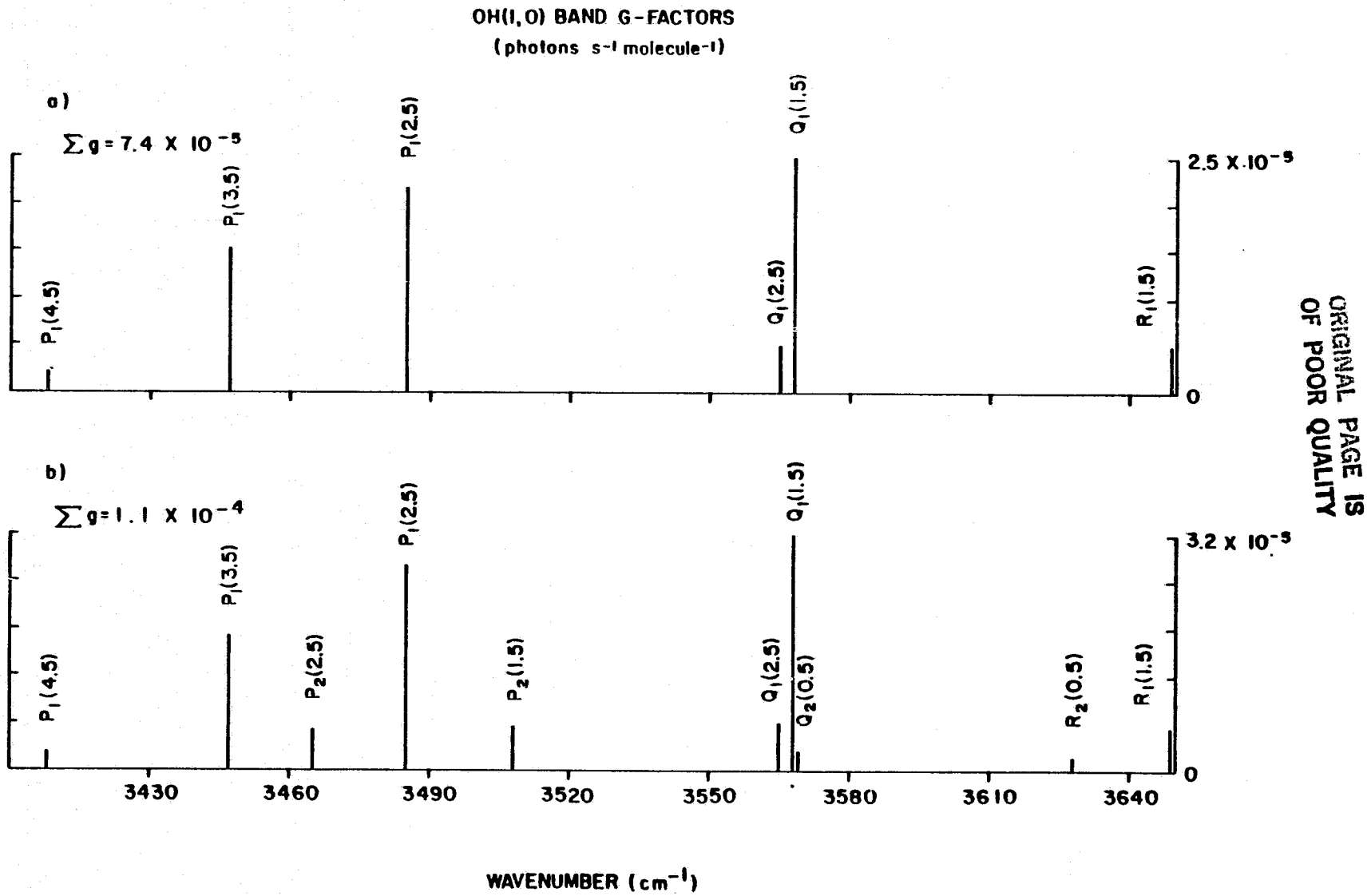

Figure 6

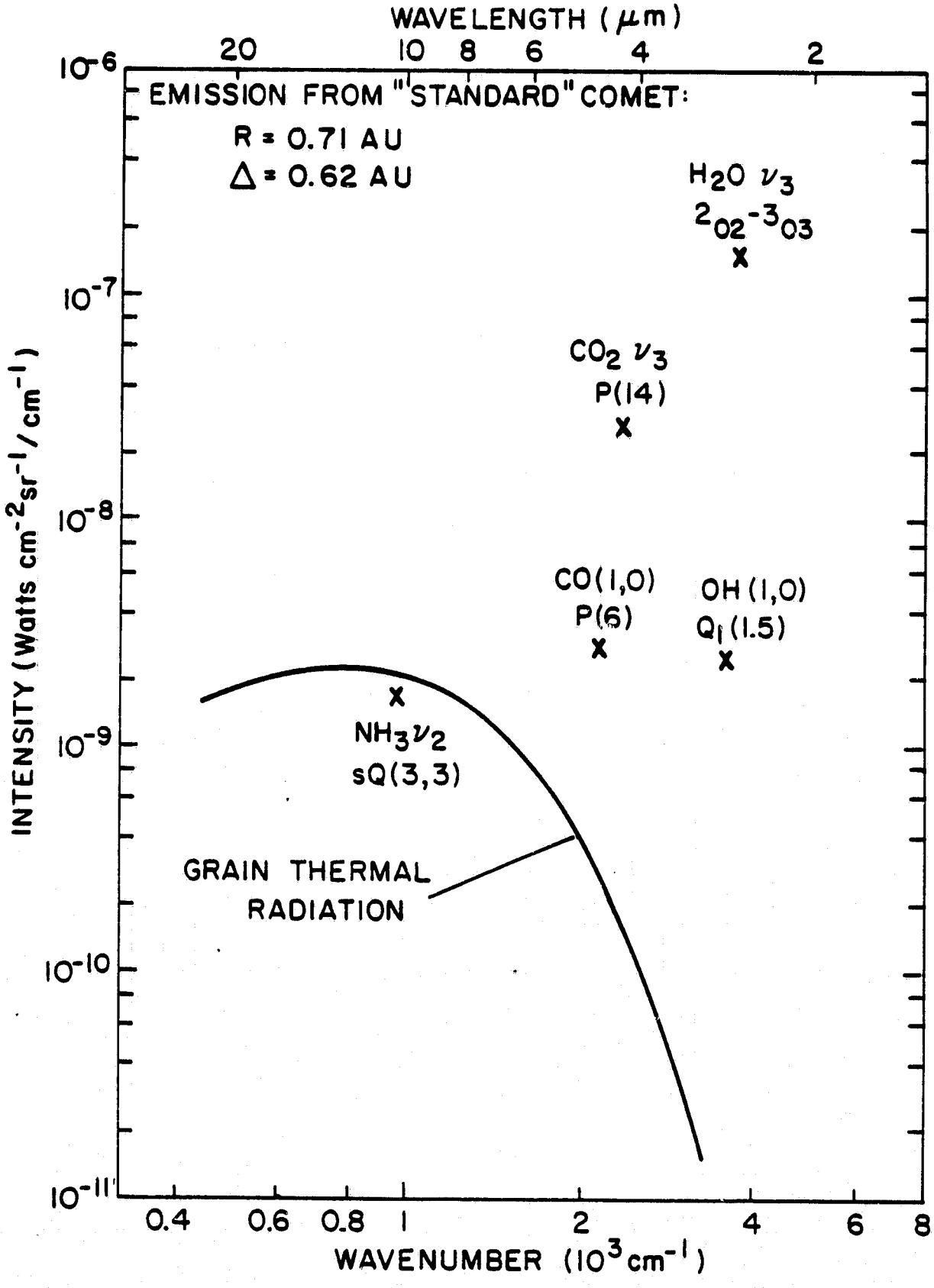

Figure 7